Submission code: R6V7GNX9B0

See this and other abstracts on our website: https://home.sbgf.org.br/Pages/resumos.php

Stiffness Tensor Data Compression Analysis in Anisotropic Seismic Modeling

Paulo Alves (UFF), Felipe Costa (GISIS/UFF), Felipe Capuzzo (GISIS / UFF), Danielle Martins Tostes (UFF), Ammir Karsou (GISIS/UFF), Rodrigo Stern (GISIS/UFF), Marco Cetale (GISIS/UFF)

SBGf Conference
18-20 NOV | Rio'25

Stiffness Tensor Data Compression Analysis in Anisotropic Seismic Modeling

This paper was prepared for presentation during the 19th International Congress of the Brazilian Geophysical Society held in Rio de Janeiro, Brazil, 18-20 November 2025. Contents of this paper were reviewed by the Technical Committee of the 19th International Congress of the Brazilian Geophysical Society and do not necessarily represent any position of the SBGf, its officers or members.

Abstract Summary

We propose a bound-normalization compression technique for the stiffness matrix in 3D general anisotropic media. This approach enables the storage of elastic coefficients using reduced memory resources. The benefits are significant, with memory usage reduced by up to 30% on the device side, while introducing only minimal errors. Seismograms generated using the compressed data remain nearly identical to those obtained without compression, confirming the effectiveness of the method.

Introduction

Three-dimensional seismic modeling in generally anisotropic media is computationally expensive due to the complexity of stress-strain relationships, particularly when media rotations are included. Okaya and McEvilly (2003) explored the effects of axis rotations on the stiffness matrix and demonstrated that, in fully anisotropic media, all 21 independent components of the stiffness tensor may be non-zero. To build the stiffness tensor we are using the weak-anisotropy formulated to orthorhombic symmetry with rotation (Thomsen, 1986; Tsvankin, 1997). The rotated finite difference staggered grid is a commonly used strategy for solving the wave equation in generally anisotropic media (Saenger et al., 2000; Zhang and Schmitt, 2025). Consequently, the objective of this study is to compress the stiffness matrix to reduce memory usage and evaluate the impact on seismogram accuracy and computational cost. We employ a comparative analysis and compute three different correlation coefficients to assess the similarity between data generated with and without compression. In terms of performance we compare results with isotropic case (Graves, 1996) without data compression memory usage.

Methodology

The stiffness matrix, representing the complete set of elastic parameters, is expressed as C_{IJ}, a 6×6 symmetric matrix with 21 independent coefficients in Voigt notation, associated with resistance to volumetric and shear deformation volumes. The compression strategy is simple, as described in the following equations

$$C'_{IJ} = 10^{-9} C_{IJ}, \tag{1}$$

$$A_{IJ} = a + (b - a) \left(\frac{C'_{IJ} - \textbf{min}(C'_{IJ})}{\textbf{max}(C'_{IJ}) - \textbf{min}(C'_{IJ})} \right), \tag{2}$$

$$C_{IJ} = 10^{9} \left(\textbf{min}(C'_{IJ}) + (A_{IJ} - a) \left(\frac{\textbf{max}(C'_{IJ}) - \textbf{min}(C'_{IJ})}{b - a} \right) \right). \tag{3}$$

Initially, the compressed volumes are loaded, and the maximum and minimum values of each normalized stiffness component C'_{IJ} are retrieved. This pre-processing step is essential to avoid costly computations within the seismic modeling kernel. Then, we multiply all the 21 independent volumes of the stiffness matrix by 10^{-9} (eq. 1), where C'_{IJ} are the rescaled elements. After that, we define boundary values between $a = 1$ and $b = 2^{16}$ (eq. 2). This bound normalization is applied to

scale the stiffness matrix into the range of a 16-bit unsigned short integer, requiring only 2 bytes per element, as opposed to 4 bytes when using the float data type. To perform wave field propagation, the physical properties must first be restored to their original scale. This is achieved by applying Equation 3 prior to each computation step. To evaluate the errors and computational overhead introduced by the proposed transformation, we conduct two three-dimensional experiments with their respective models, as shown in Figure 1. The first test involves a homogeneous model with a fully populated stiffness matrix (eq. 4), defined over a domain of 3 km in each spatial direction (see Fig. 1a). The homogeneous coefficients are described below

$$C_{IJ} = \begin{bmatrix} 1.29996426 & 0.58337507 & 0.58579036 & -0.00001265 & -0.00170636 & 0.00000893 \\ & 1.29999100 & 0.58578803 & 0.00085316 & 0.00002527 & 0.00000893 \\ & & 1.00003750 & 0.00070482 & -0.00143497 & -0.00000155 \\ & & & 0.27563484 & 0.00000311 & -0.00086582 \\ & & & & 0.27563011 & 0.00043288 \\ & & & & & 0.35830117 \end{bmatrix} \times 10^9. \quad (4)$$

The second test considers a layered model exhibiting vertical transverse isotropy, characterized by the parameters ϵ, δ and γ, as defined by Thomsen (1986). The model spans dimensions of $(x, y, z) = (5, 5, 2)$ km. Figure 1 presents the elastic properties for each layer, 100 meters in thickness, displayed in well logs for velocity, density, and anisotropic parameters. The two models are discretized with a regular grid spacing of 12.5 m. We employ a classical absorbing boundary condition with a thickness of 50 samples, over 1.5 propagation seconds, using a time increment of 1 ms. The acquisition geometry for each experiment consists of a single source. In the homogeneous model, the source is positioned at the center of the domain, while in the layered model, it is located at the center of the surface. In the homogeneous experiment, 40 receivers are deployed at a depth of 200 meters, spaced 50 meters apart. In the layered model, 100 receivers are used with the same aspects.

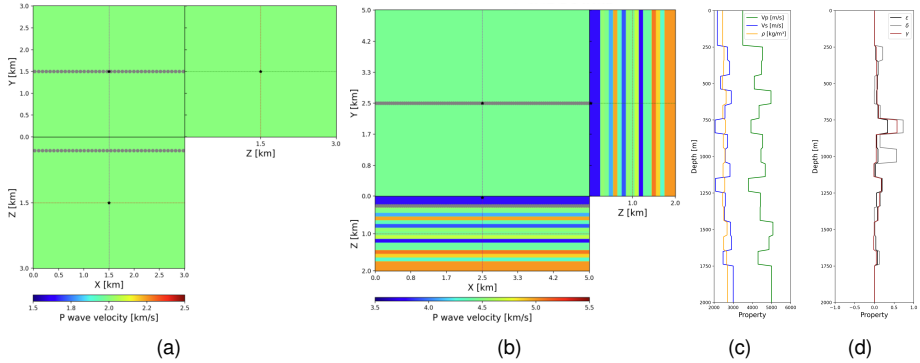

Figure 1: Model to simulate the compression experiment where source is the black dot and receivers are gray dots. (a) The homogeneous model with 21 non-zero components with its stiffness matrix defined by equation 4. (b) The layered model defined by properties described in Thomsen (1986). (c) and (d) are well logs for velocities, density and anisotropic parameters.

Results

Results are organized in terms of seismograms and their corresponding differences, benchmark tables, and a summary of correlation coefficients. The experiments were conducted on a system equipped with an Intel Core i7-12700 CPU and a NVIDIA RTX 3060 GPU. Figure 2 illustrates the outcomes of the first experiment. As shown in Fig. 2(c), the difference between the compressed and standard methodologies is negligible. Observable differences emerge only when the amplitude

threshold is reduced to 0.001% of the original seismogram's maximum amplitude. Additionally, Table 1 reveals a memory reduction of 18% on the host and 32% on the device achieved through the proposed compression methodology, that brings the memory usage closer to the simplified isotropic case.

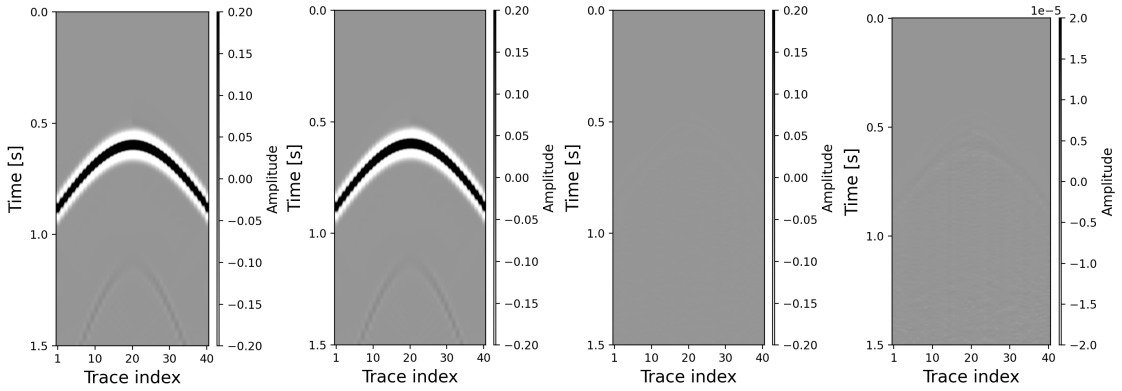

Figure 2: Seismograms and their corresponding differences obtained from the homogeneous model experiment. (a) The compressed and (b) the no compressed stiffness result. (c) The difference between them at the same scale and (d) the difference rescaled to 0.001% of the original scale.

Table 1: Benchmarks for homogeneous model.

	Anisotropic		Isotropic
	no Compression	Compression	Simplified formulation
Runtime	60.2 s	55.4 s	36.5 s
RAM Usage	2308 MB	1877 MB	1382 MB
GPU Usage	5234 MB	3538 MB	2246 MB

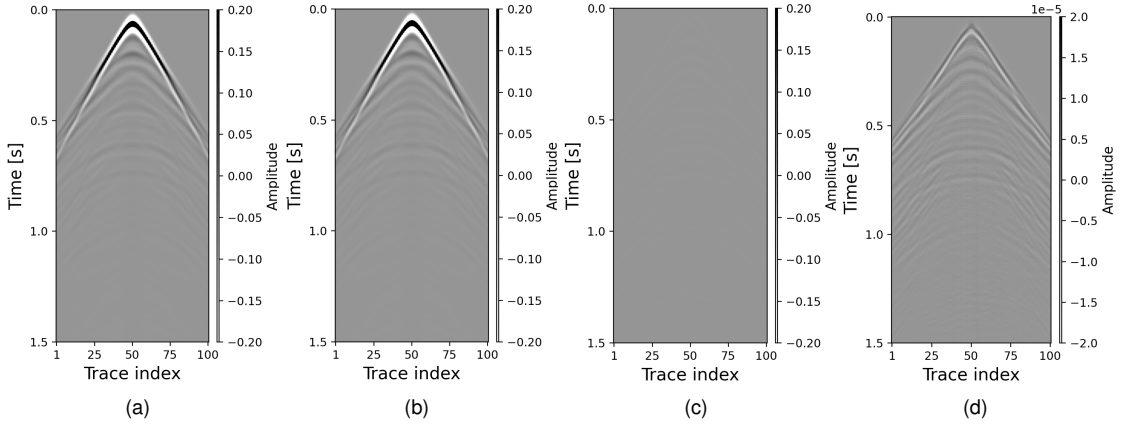

Figure 3: Seismograms and their corresponding differences obtained from the layered model experiment. (a) The compressed and (b) the no compressed stiffness result. (c) The difference between them at the same scale and (d) the difference rescaled to 0.001% of the original scale.

Figure 3 presents the results of the second experiment. As shown in Fig. 3(c), the difference between the compressed and standard methodologies is minimal. Observable discrepancies only

appear when the amplitude threshold is reduced to 0.001% of the original seismogram's maximum amplitude. Furthermore, Table 2 reveals a memory reduction of 20% on the host and 30% on the device, achieved through the proposed compression methodology, bringing memory usage closer to that of the simplified isotropic case formulation without compression.

Table 2: Benchmarks for layered model.

	Anisotropic		Isotropic
	no Compression	Compression	Simplified formulation
Runtime	122.5 s	110.8 s	76.5 s
RAM Usage	4032 MB	3220 MB	2255 MB
GPU Usage	8460 MB	5858 MB	3710 MB

Table 3 presents popular correlation strategies: Pearson, Spearman, and Kendall, correlation coefficients, used to assess the similarity between seismograms generated with and without compression in both experiments. A correlation coefficient closer to one indicates higher similarity. All metrics confirm a strong agreement, demonstrating that the compressed seismograms are nearly identical to those obtained without compression.

Table 3: Comparison of correlation coefficients for homogeneous and layered model experiment.

	Homogeneous Model	Layered Model
Pearson	0.9999	0.99999
Spearman	0.9998	0.99997
Kendall	0.9996	0.99976

Conclusions

We developed a methodology to compress the elastic tensor in generally anisotropic seismic modeling. This approach significantly reduces memory usage, by up to 30% on the device, while maintaining the seismograms accuracy. The resulting errors are minimal, with seismograms showing near-identical responses to those computed using uncompressed properties, as confirmed by high correlation coefficients. This compression strategy enables more efficient use of computational resources without sacrificing the fidelity of the physical modeling.

Acknowledgments

The authors from Fluminense Federal University acknowledge the financial support from Petrobras through the R&D project *Modelagem Visco-Elástica Anisotrópica em dados Multi-Azimutais para Análise de Sensibilidade de Sistemas de Fraturas* (ANP nº 24643-9). The strategic importance of the R&D levy regulation of the National Agency for Petroleum, Natural Gas and Biofuels (ANP) is gratefully appreciated. We would like to thank Mr. Rodrigo Stern (GISIS/UFF) for the IT support.

References

Graves, R. W., 1996, Simulating seismic wave propagation in 3D elastic media using staggered-grid finite differences: Bulletin of the Seismological Society of America, **86**, 1091–1106.

Okaya, D. A., and T. V. McEvilly, 2003, Elastic wave propagation in anisotropic crustal material possessing arbitrary internal tilt: Geophysical Journal International, **153**, 344–358.

Saenger, E. H., N. Gold, and S. A. Shapiro, 2000, Modeling the propagation of elastic waves using a modified finite-difference grid: Wave Motion, **31**, 77–92.

Thomsen, L., 1986, Weak elastic anisotropy: Geophysics, **51**, 1954–1966.

Tsvankin, I., 1997, Anisotropic parameters and P-wave velocity for orthorhombic media: Geophysics, **62**, 1292–1309.

Zhang, O., and D. R. Schmitt, 2025, An optimized 2d/3d finite-difference seismic wave propagator using rotated staggered grid for complex elastic anisotropic structures: Computers & Geosciences, **196**.